

# Influence of Nd doping on microwave dielectric properties of SrTiO<sub>3</sub> ceramics

Wenjie Bian<sup>1,2,3</sup> · Xiaochi Lu<sup>1,2,3</sup> · Yaoyao Li<sup>1,2,3</sup> · Chengfa Min<sup>1,2,3</sup> · Haikui Zhu<sup>1,2,3</sup> · Zhenxiao Fu<sup>1,3</sup> · Qitu Zhang<sup>1,3</sup>

Received: 29 September 2017 / Accepted: 3 November 2017  
© Springer Science+Business Media, LLC, part of Springer Nature 2017

**Abstract** Sr<sub>1-x</sub>Nd<sub>x</sub>TiO<sub>3</sub> ( $x = 0.08\text{--}0.14$ ) ceramics were prepared by conventional solid-state methods. The analysis of crystal structure suggested Sr<sub>1-x</sub>Nd<sub>x</sub>TiO<sub>3</sub> ceramics appeared to form tetragonal perovskite structure. The relationship between charge compensation mechanism, microstructure feature and microwave dielectric properties were investigated. Trivalent Nd<sup>3+</sup> substituting Sr<sup>2+</sup> could effectively decrease oxygen vacancies. This reduction and relative density were critical to improve  $Q \times f$  values of Sr<sub>1-x</sub>Nd<sub>x</sub>TiO<sub>3</sub> ceramics. For  $\epsilon_r$  values, incorporation of Nd could restrain the rattling of Ti<sup>4+</sup> cations and led to the reduction of dielectric constant. The  $\tau_f$  values were strongly influenced by tilting of oxygen octahedral. The  $\tau_f$  values decreased from 883 to 650 ppm/°C with  $x$  increasing from 0.08 to 0.14. A better microwave dielectric property was achieved for composition Sr<sub>0.92</sub>Nd<sub>0.08</sub>TiO<sub>3</sub> at 1460 °C:  $\epsilon_r = 160$ ,  $Q \times f = 6602$  GHz,  $\tau_f = 883$  ppm/°C.

## 1 Introduction

In recent years, owing to miniaturization and high quality of microwave communication equipment, microwave dielectric ceramics with high dielectric constant and low loss factor play important roles in microwave microelectronic devices

[1–3]. Because of high dielectric constant, the perovskite-type titanates, such as CaTiO<sub>3</sub> and SrTiO<sub>3</sub>, have attracted more attention as microwave dielectric materials [4, 5]. However, high positive frequency temperature coefficient is a serious problem to be solved.

SrTiO<sub>3</sub> ceramic, a typical cubic perovskite type ceramic, has relatively high dielectric constant  $\epsilon_r$  (~300) and  $Q \times f$  value (~3000 GHz), but large positive frequency temperature coefficient  $\tau_f$  (~1650 ppm/°C) limits their practicality [6, 7]. In order to be widely used, researchers improve dielectric properties of SrTiO<sub>3</sub> ceramics by adjusting the sintering process, doping, changing the stoichiometric ratio and sintering atmosphere [8, 9].

Improving dielectric properties of SrTiO<sub>3</sub> ceramics by substituting Sr<sup>2+</sup> ions or Ti<sup>4+</sup> ions has caught researchers' attention. In general, ions with smaller radius and higher valence tend to substitute Ti<sup>4+</sup>. On the contrary, ions with larger radius and lower valence tend to substitute Sr<sup>2+</sup>. However, for rare earth (RE) ions, the positions where rare earth ions occupy are related to their radius size and concentration [10]. If the radius or doping concentration of rare earth ions are smaller, rare earth ions will substitute Sr<sup>2+</sup> ions. Or rare earth ions will substitute Ti<sup>4+</sup> ions.

For SrTiO<sub>3</sub> ceramics, oxygen vacancies can be induced by loss of oxygen from the crystal lattice when sintered at high temperatures [11]. Oxygen vacancies can generate anharmonic vibration and thus can cause extrinsic dielectric loss [12]. Researchers find that trivalent ions, such as Bi<sup>3+</sup>, La<sup>3+</sup>, Pr<sup>3+</sup>, Ce<sup>3+</sup> and Nd<sup>3+</sup>, doped SrTiO<sub>3</sub> ceramics can cause electric unbalance [13–19]. The electric unbalance can be compensated by inducing Sr or Ti vacancies. These cation vacancies can react with the oxygen vacancies to reduce the number of oxygen vacancies [20].

SrTiO<sub>3</sub> ceramics were rarely reported in the microwave application due to the large positive frequency temperature

✉ Qitu Zhang  
ngdzqt@163.com

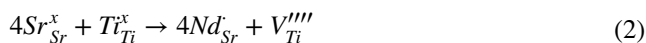
<sup>1</sup> College of Materials Science and Engineering, Nanjing Tech University, Nanjing 210009, China

<sup>2</sup> Jiangsu Collaborative Innovation Center for Advanced Inorganic Function Composites, Nanjing 210009, China

<sup>3</sup> Fenghua Advanced Technology Holding Co Ltd, Zhaoqing 526000, China

coefficient. Effect of structural changes in perovskites on frequency temperature coefficient is a key to solve this problem. As reported by Collar et al. [21], the octahedral tilting will affect  $\tau_f$ . The  $\tau_f$  moves towards negative as the tilting increases. Rare earth ions doping has an effect on the octahedral tilting. Fu Maosen et al. [22] reports that Nd doping  $\text{CaTiO}_3$  ceramics can effectively increase octahedral tilting and decrease positive frequency temperature coefficient.

In this work, we chose  $\text{Nd}_2\text{O}_3$  to improving dielectric properties  $\text{SrTiO}_3$  ceramics.  $\text{Nd}^{3+}$  doping into Sr-site will cause electric unbalance. The electric unbalance can be compensated by inducing Sr or Ti vacancies by following equations:



For donor-doped  $\text{SrTiO}_3$  ceramics, there is still much disputation left from the cation vacancies charge compensation point of view. The charge compensation mechanism is complicated. Shen Zongyang [23] reported that the internal charge compensation mechanism is belong to “self-compensation mechanism”, which causes Nd or Ti partially gathering together in the grain boundary. So Nd donor-doped  $\text{SrTiO}_3$  ceramics will induce Sr and Ti vacancies.

Doping  $\text{Nd}^{3+}$  can effectively improve  $Q \times f$  values and tune frequency temperature coefficient of  $\text{SrTiO}_3$  ceramics. We discuss the effects of  $\text{Nd}^{3+}$  substitution on the dielectric properties. The factors such as densification, octahedral tilting, rattling of  $\text{Ti}^{4+}$  cations in the octahedral site, etc. are discussed in this work.

## 2 Experimental

$\text{Sr}_{1-x}\text{Nd}_x\text{TiO}_3$  ceramics were prepared by conventional solid-state methods.  $\text{Nd}_2\text{O}_3$  was added into  $\text{SrCO}_3$  and  $\text{TiO}_2$  to synthesize the  $x$  mol% Nd doped  $\text{SrTiO}_3$  ceramics, where  $x = 0.08, 0.10, 0.12, 0.14$ . The mixtures were ground for 8 h in a Nylon bottle with deionized water and agate balls. After dried, the prepared powders were calcined at 1200 °C for 3 h. Then the calcined powders were ball-milled for 8 h and dried. Next, the powders were milled with 7 wt% of PVA as a binder and were pressed into cylindrical pellets of 13 mm in diameter and 6–6.5 mm in thickness under 2 MPa. These pellets were sintered at 1380–1500 °C for 3 h in air.

The phase composition of the sintered samples were identified by X-ray diffraction (RigakuD/Max 2500 type, Japan) with  $\text{Cu K}\alpha$  radiation ( $k = 0.15406$  nm with 2 h step 0.02). The microstructural observations and surface microstructures of the sintered samples were performed by scanning electron microscope (SEM, Hitachi SU8010, Japan).

The bulk densities of ceramic samples were tested by Archimedes method. Moreover, the microwave dielectric properties ( $\epsilon_r$  and  $Q \times f$ ) were measured by means of the Hakki and Coleman and Courtney method using a Network Analyzer (Agilent E5071C, Malaysia). The  $\tau_f$  values were measured by using high and low temperature test chamber at the temperature range from 20 to 80 °C, and calculated by the formula (3).

$$\tau_f = \frac{f_2 - f_1}{f_1(T_2 - T_1)} \quad (3)$$

$f_2, f_1$  were the resonant frequencies at the measuring temperature  $T_2$  (80 °C) and  $T_1$  (20 °C), respectively.

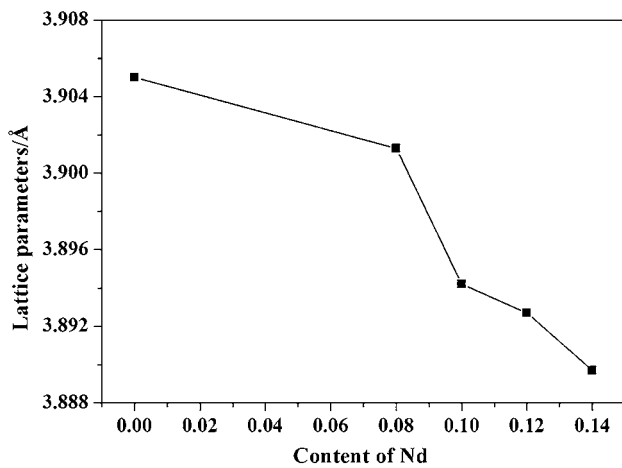
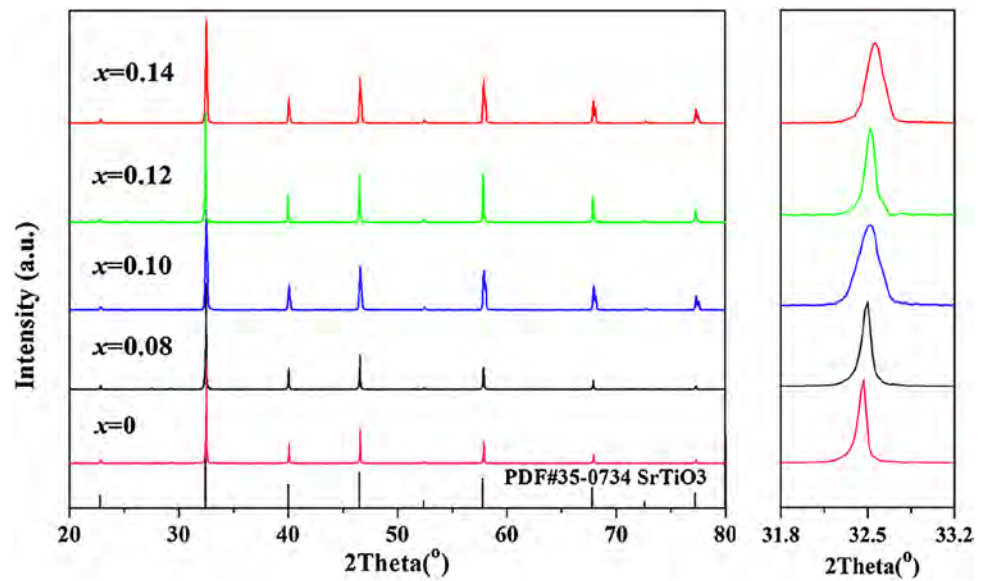
## 3 Results and discussion

Figure 1 shows XRD patterns of  $\text{Sr}_{1-x}\text{Nd}_x\text{TiO}_3$  ( $x = 0.08\text{--}0.14$ ) ceramics with different  $x$  values. It was clear that all ceramic samples had tetragonal perovskite structure and the patterns were similar to  $\text{SrTiO}_3$  ceramics with no additional peaks. It demonstrated that Nd doped into the host lattice of  $\text{SrTiO}_3$  and samples formed  $\text{Sr}_{1-x}\text{Nd}_x\text{TiO}_3$  solid solution from  $x = 0.08$  to  $x = 0.14$ . The diffraction peaks at 31.8°–33.2° slightly shifted to higher angles with Nd doping concentrations increasing. The ionic radius of  $\text{Nd}^{3+}$  ion ( $r_{\text{Nd}^{3+}} = 0.98$  Å) are smaller than those of the  $\text{Sr}^{2+}$  ion ( $r_{\text{Sr}^{2+}} = 1.18$  Å). Nd doping into Sr-site caused the shrinkage of the lattice. This phenomenon also suggested that Nd doped into the host lattice of  $\text{SrTiO}_3$ . The variation of lattice parameters correspond to this shrinkage of the lattice from  $a = 3.905$  Å at  $x = 0$  to  $a = 3.8897$  Å at  $x = 0.14$ , which was observed in Fig. 2.

Figure 3 shows the SEM of  $\text{Sr}_{1-x}\text{Nd}_x\text{TiO}_3$  ceramics with different  $x$  values. As seen from Fig. 3, samples had dense microstructures. The SEM images revealed that the grain size slightly decreased when content of Nd was added. The average grain size of  $\text{SrTiO}_3$  ceramics was about 30 µm. As Fig. 3a shows, when  $x = 0.08$ , the average grain size of  $\text{Sr}_{1-x}\text{Nd}_x\text{TiO}_3$  ceramics decreased to about 1 µm. Then, the average grain size of  $\text{Sr}_{1-x}\text{Nd}_x\text{TiO}_3$  ceramics decreased with the growing content of Nd. It suggested that incorporation of Nd inhibited the growth of grains size. The inhibition of gain size was due to the existence of Nd or Ti at the grain boundary. The doping mechanism indicated that Nd substitution induced Sr and Ti vacancies into the ceramic system. What's more, as Fig. 3 shows, further Nd substitution resulted in irregular grain and uneven grain size.

Variations of the relative densities of the  $\text{Sr}_{1-x}\text{Nd}_x\text{TiO}_3$  ( $x = 0.08\text{--}0.14$ ) ceramics at different sintering temperature are shown in Fig. 4. When the sintering temperature was 1380 °C, the relative densities were less than 80%. The

**Fig. 1** XRD patterns of  $\text{Sr}_{1-x}\text{Nd}_x\text{TiO}_3$  ceramics with different  $x$  value range from 20° to 80° and 31.8° to 33.2°



**Fig. 2** Lattice parameters of  $\text{Sr}_{1-x}\text{Nd}_x\text{TiO}_3$  ceramics doped with different Nd content

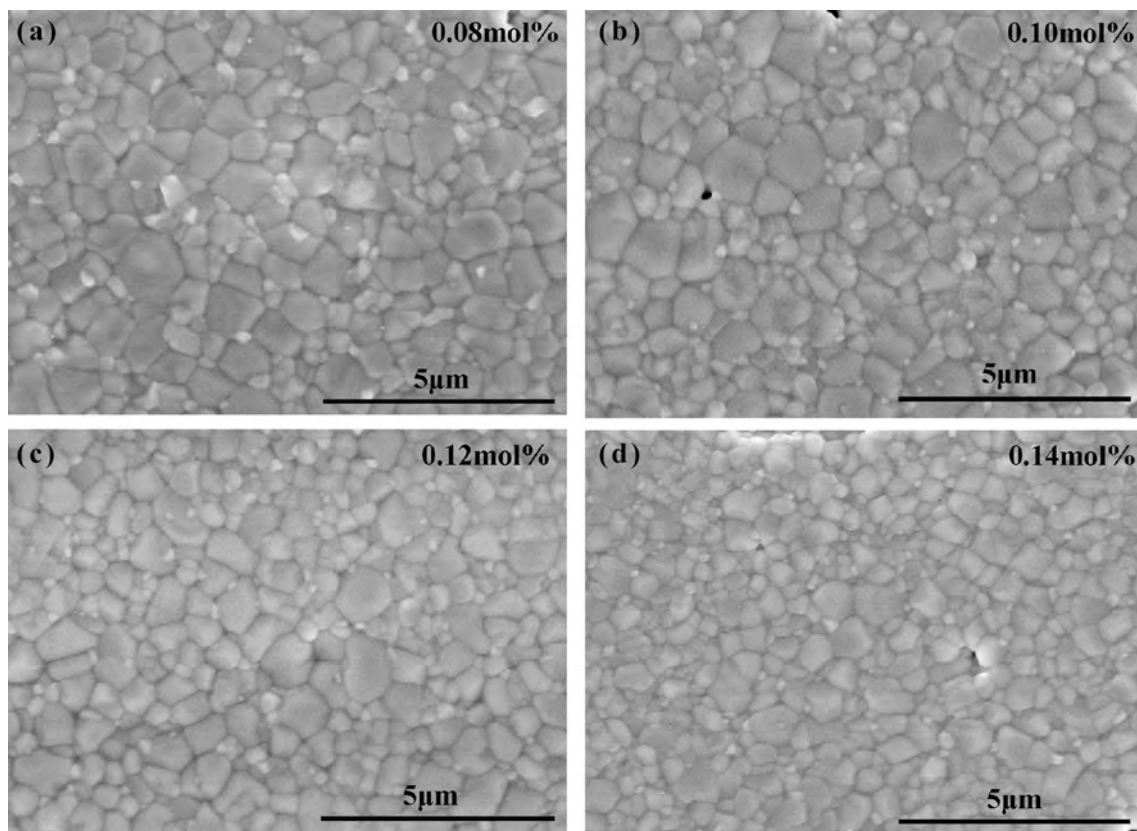
relative densities of ceramics rose rapidly with the sintering temperature increased. When the sintering temperature was 1460 °C, the relative density of ceramics reached a maximum, 96%, at  $x=0.08$ . So, from the point of densification, the best sintering temperature was 1460 °C. Then the relative density of ceramics began to decrease. When the sintering temperature exceeded 1460 °C, the abnormal grain growth occurred. In addition, the relative density of ceramics decreased slightly with the growing content of Nd, sintered at 1460 °C. But the relative densities of ceramics were still above 92%. Therefore, at this range of Nd substitution, the relative density is independent of Nd content.

Figure 5 shows dielectric constant of the  $\text{Sr}_{1-x}\text{Nd}_x\text{TiO}_3$  ( $x=0.08-0.14$ ) ceramics at different sintering temperature. Comparing with  $\text{SrTiO}_3$  ceramics (~300),  $\epsilon_r$  values of the  $\text{Sr}_{1-x}\text{Nd}_x\text{TiO}_3$  ceramics were under 166.  $\epsilon_r$  values

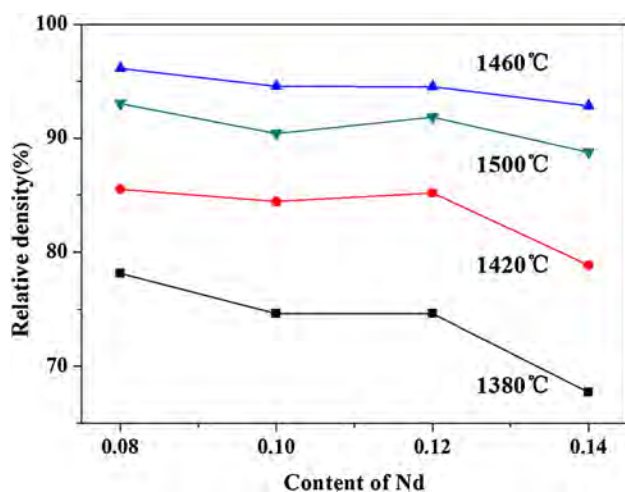
reached a maximum value of 166, at  $x=0.08$ , sintered at 1420 °C. Then  $\epsilon_r$  values of ceramics decreased sharply with the increasing content of Nd. Incorporation of Nd reduced  $\epsilon_r$  values of the  $\text{Sr}_{1-x}\text{Nd}_x\text{TiO}_3$  ceramics effectively. It is reported that high dielectric constant of  $\text{SrTiO}_3$  is attributed to the rattling of  $\text{Ti}^{4+}$  cations in the oxygen octahedral [24]. Incorporation of Nd could restrain the rattling of  $\text{Ti}^{4+}$  cations [22] and lead to the decreasing of dielectric constants. When sintered at 1380 °C, the relative densities were low and caused lower dielectric constants, which was due to the existence of air.

Figure 6 shows  $Q \times f$  values of the  $\text{Sr}_{1-x}\text{Nd}_x\text{TiO}_3$  ( $x=0.08-0.14$ ) ceramics at sintering temperature range from 1380 to 1500 °C. When sintered at 1380 and 1420 °C, the  $Q \times f$  values were relatively low, which was due to lower densification of ceramics. The  $Q \times f$  values decreased from 6602 to 5631 GHz, sintered at 1460 °C, with the content of Nd increased. Comparing with  $\text{SrTiO}_3$  ceramics (~3000 GHz), incorporation of Nd can improve  $Q \times f$  values of ceramics. Sr or Ti vacancies, generated by incorporation of Nd, effectively decreased oxygen vacancies which can generate extrinsic dielectric loss and improve  $Q \times f$  values of ceramics. Further Nd substitution resulted in irregular grain and uneven grain size, which had a bad effect on  $Q \times f$  values of ceramics.

The variations in frequency temperature coefficient and tolerance factor  $t$  of the  $\text{Sr}_{1-x}\text{Nd}_x\text{TiO}_3$  ceramics as a function of  $x$ , sintered at 1460 °C, are shown in Fig. 7. The  $\tau_f$  values of ceramics decreased from 883 to 650 ppm/°C, with  $x$  increasing from 0.08 to 0.14. Comparing with  $\text{SrTiO}_3$  ceramics (~1650 ppm/°C), incorporation of Nd obviously decreased  $\tau_f$  values of ceramics, which was consistent with the research of Reany [25, 26]. In their report, the  $\tau_f$  values moves toward negative in the  $t < 1$



**Fig. 3** SEM images of  $\text{Sr}_{1-x}\text{Nd}_x\text{TiO}_3$  ceramics with **a**  $x=0.08$ , **b**  $x=0.10$ , **c**  $x=0.12$ , **d**  $x=0.14$ , sintered at  $1460^\circ\text{C}$



**Fig. 4** Relative densities of the  $\text{Sr}_{1-x}\text{Nd}_x\text{TiO}_3$  ( $x=0.08\text{--}0.14$ ) ceramics at different sintering temperature

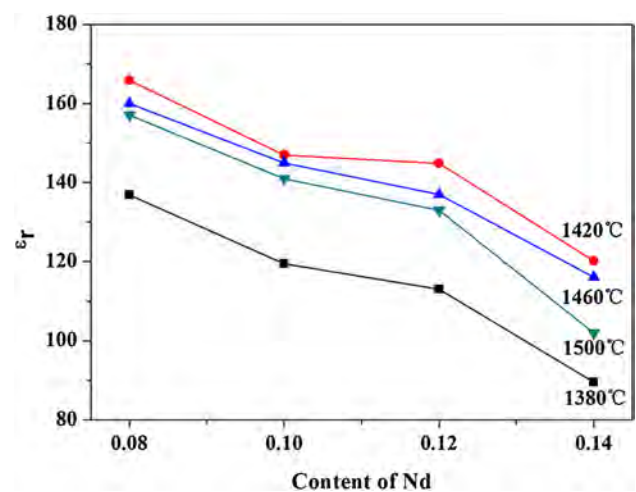


**Fig. 5** Dielectric constant of the  $\text{Sr}_{1-x}\text{Nd}_x\text{TiO}_3$  ( $x=0.08\text{--}0.14$ ) ceramics at different sintering temperature

region of perovskite structure as tilting of oxygen octahedral increases. As Fig. 7b shows, tolerance factor  $t$  decreased. It indicated that the tilting of oxygen octahedral increased. Therefore, the  $\tau_f$  values moved toward negative and decreased sharply.

#### 4 Conclusion

$\text{Sr}_{1-x}\text{Nd}_x\text{TiO}_3$  ceramics were synthesized by a conventional solid-state method. The structural analysis suggested that  $\text{Nd}^{3+}$  ions entered the  $\text{SrTiO}_3$  crystal lattice and samples



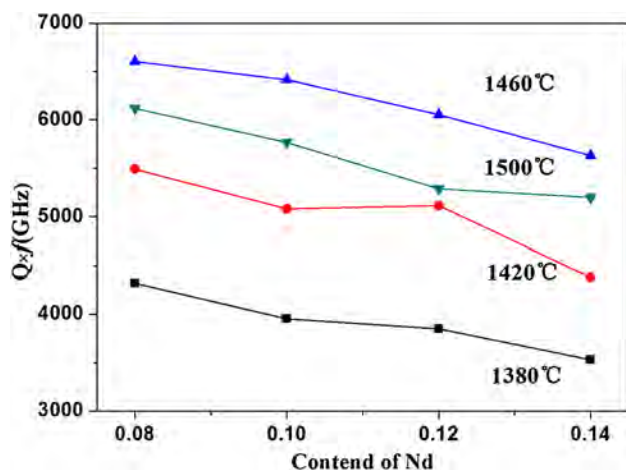


**Fig. 6**  $Q \times f$  values of the  $\text{Sr}_{1-x}\text{Nd}_x\text{TiO}_3$  ( $x=0.08\text{--}0.14$ ) ceramics varied with  $x$  and sintering temperatures

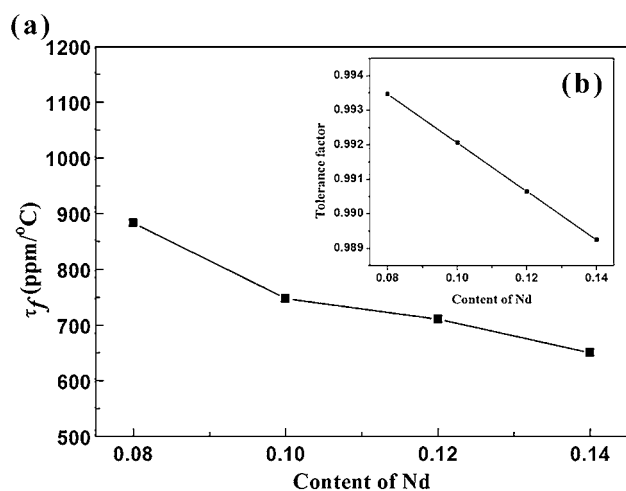


**Fig. 7** Variations in frequency temperature coefficient and tolerance factor  $t$  of the  $\text{Sr}_{1-x}\text{Nd}_x\text{TiO}_3$  ( $x=0.08\text{--}0.14$ ) ceramics as a function of  $x$ , sintered at 1460 °C

formed  $\text{Sr}_{1-x}\text{Nd}_x\text{TiO}_3$  solid solution with single perovskite structure from  $x=0.08$  to  $x=0.14$ . The morphological analysis indicated incorporation of Nd inhibited the growth of grains. From the point of densification, the best sintering temperature was 1460 °C. Degree of densification had an obviously influence on dielectric properties of ceramics.  $\text{Nd}^{3+}$  donor-doping into Sr-site can weaken the bad influence caused by oxygen vacancies on  $Q \times f$  values. When  $x=0.08$ , the  $Q \times f$  values reached a maximum value of 6602 GHz. For  $\epsilon_r$ , incorporation of Nd caused  $\epsilon_r$  values decreased. The  $\tau_f$  values are related to tilting of oxygen octahedral. Incorporation of Nd caused tilting of oxygen octahedral increasing. The  $\tau_f$  values decreased from 883 to 650 ppm/°C with the growing content of Nd. The  $\tau_f$  is still large and is worthy of

further study. In a word, incorporation of Nd is a promising way to improve microwave dielectric properties of  $\text{SrTiO}_3$  ceramics.

**Acknowledgements** This work was supported by Priority Academic Program Development of Jiangsu Higher Education Institutions (PAPD), the Opening Project of the State Key Laboratory of High-Performance Ceramics and Superfine Microstructure (Project No. SKL201309SIC), the College Industrialization Project of Jiangsu Province (JHB2012-12), the Jiangsu Collaborative Innovation Center for Advanced Inorganic Function Composites, the Science and Technology Projects of Guangdong Province (Project No. 2011A091103002).

## References

1. M.T. Sebastian, *Dielectric Materials for Wireless Communication*. (Elsevier, Oxford, 2008)
2. C.L. Huang, C.F. Tseng, W.R. Yang, T.J. Yang, *J. Am. Ceram. Soc.* **91**(7), 2201–2204 (2008)
3. Y.Y. Li, X.C. Lu, Y. Zhang et al., *Ceram. Int.* **43**(14), 11516–11522 (2017)
4. Y. Okamoto, Y. Suzuki, *J. Ceram. Soc. Jpn.* **122**(1428), 728–731 (2014)
5. W. Wang, L. Tang, W. Bai, B. Shen, J. Zhai, *J. Mater. Sci.: Mater. Electron.* **25**(8), 3601–3607 (2014)
6. Z.Y. Shen, Q.G. Hu, Y.M. Li et al., *J. Mater. Sci.: Mater. Electron.* **24**(8), 3089–3094 (2013)
7. F. Liu, C. Yuan, X. Liu, G. Chen, C. Zhou, J. Qu, *Mater. Chem. Phys.* **148**(3), 1083–1088 (2014)
8. Z. Wang, M. Cao, Z. Yao et al., *Ceram. Int.* **40**(1), 929–933 (2014)
9. A. Tkach, P.M. Vilarinho, A.L. Kholkin, *Acta. Mater.* **54**(20), 5385–5391 (2006)
10. A. Tkach, T.M. Correia, A. Almeida et al., *Acta. Mater.* **59**(14), 5388–5397 (2011)
11. C.C. Wang, C.M. Lei, G.J. Wang et al., *J. Appl. Phys.* **113**(9), 392 (2013)
12. R.C. Pullar, S.J. Penn, X. Wang, I.M. Reaney, N.M. Alford, *J. Eur. Ceram. Soc.* **29**(3), 419–424 (2009)
13. A. Chen, Y. Zhi, *J. Appl. Phys.* **71**(12), 6025–6028 (1992)
14. L. Liu, Y. Wang, Y. Bai et al., *Mater. Trans.* **37**(2), 142–149 (1996)
15. W.Q. Luo, Z.Y. Shen, Y.M. Li, Z.M. Wang, R.H. Liao, X.Y. Gu, *J. Electroceram.* **31**(1–2), 117–123 (2013)
16. C. Ang, Z. Yu, *Appl. Phys. Lett.* **88**(16), 474 (2006)
17. Y. Zhi, A. Chen, *J. Mater. Sci.* **38**(1), 113–118 (2003)
18. A. Durán, E. Martínez, J.A. Díaz, J.M. Siqueiros, *J. Appl. Phys.* **97**(10), 677 (2005)
19. B. Ullah, W. Lei, X.Q. Song et al., *J. Alloys Compd.* **728**, 623–630 (2017)
20. L. Wang, Y. Sakka, S. Yang, G.A. Botton, T. Kolodiazny, *J. Am. Ceram. Soc.* **93**(9), 2903–2908 (2010)
21. E.L. Colla, I.M. Reaney, N. Setter, *J. Appl. Phys.* **74**(5), 3414–3425 (1993)
22. M.S. Fu, X.Q. Liu, X.M. Chen, *J. Eur. Ceram. Soc.* **28**(3), 585–590 (2008)
23. Z.Y. Shen, Y.M. Li, W.Q. Luo, Z.M. Wang, X.Y. Gu, R.H. Liao, *J. Mater. Sci. Mater. Electron.* **24**(2), 704–710 (2013)
24. E.R. Kipkoech, F. Azough, R. Freer, *J. Appl. Phys.* **97**(6), 715 (2005)
25. I.M. Reaney, P. Wise, R. Ubbelohde et al., *Philos. Mag.* **81**(2), 501–510 (2001)
26. I.M. Reaney, E.L. Colla, N. Setter, *Jpn. J. Appl. Phys.* **33**(7A), 3984–3990 (1994)